Silica-Coated Magnetic-Nanoparticle-Supported DABCO-Derived Acidic Ionic Liquid for the Efficient Synthesis of Bioactive 3,3-Di(indolyl)indolin-2-ones

Radhika Gupta,[†] Manavi Yadav,[†,‡] Rashmi Gaur,[†,§] Gunjan Arora,[†] Pooja Rana,[†] Priya Yadav,[†,‡] Alok Adholeya,[∥] and Rakesh K. Sharma*,[†]

[†]Green Chemistry Network Centre, Department of Chemistry and [‡]Department of Chemistry, Hindu College, University of Delhi, Delhi 110007, India

[§]Department of Chemistry, J. C. Bose University of Science & Technology, YMCA, Faridabad 121006, Haryana, India

[∥]TERI-Deakin Nanobiotechnology Centre, TERI Gram, The Energy and Resources Institute, Gurugram 122102, India

Ⓢ Supporting Information

ABSTRACT: In this work, biologically significant 3,3-di(indolyl)indolin-2-ones have been synthesized using a silica-coated magnetic-nanoparticle-supported 1,4-diazabicyclo[2.2.2]-octane (DABCO)-derived and acid-functionalized ionic liquid as the catalytic entity. The fabricated nanocomposite catalyzes the pseudo-three-component reaction of isatins and indoles explicitly via hydrogen-bonding interactions between substrates and the catalyst. The nanocatalytic system utilizes water as the green reaction medium to obtain a library of indolinones in good to excellent yields under mild reaction conditions. Besides, the catalyst could be easily recovered from the reaction mixture through simple external magnetic forces, which enables excellent recyclability of the catalyst for successive runs without appreciable loss in catalytic activity. Hence, the outcomes of the present methodology make the nanocatalyst a potential candidate for the development of green and sustainable chemical processes.
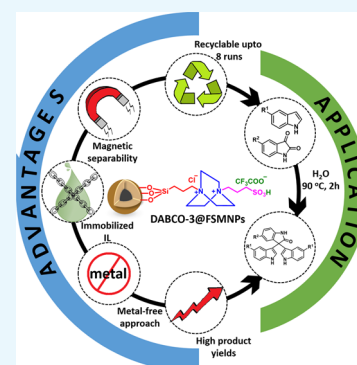
INTRODUCTION

3,3-Di(indolyl)indolin-2-ones are one of the privileged heterocyclic molecules that possess potential biological efficacies, including spermicidal (Figure 1a),[1] anticancer,[2,3] and α-glucosidase inhibitory properties (Figure 1b).[4] One such motif, namely, trisindoline, has also shown considerable activity t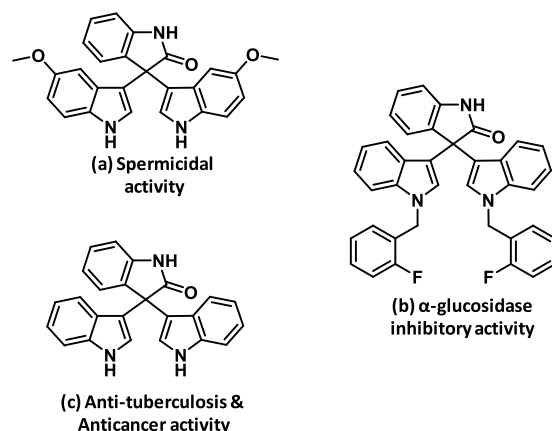o inhibit *Micobacterium tuberculosis* strain H37Rv[5] and cytotoxic effect against both parental and multidrug-resistant cancerous cells (Figure 1c).[6]

Due to these fascinating biological properties, a repertoire of methods have been developed for the synthesis of 3,3-di(indolyl)indolin-2-ones, each involving the participation of indoles and isatins as synthons via a pseudo-three-component reaction. In this context, numerous metal salts and complexes, such as Bi(OTf)$_3$,[7] Zn(OTf)$_2$,[8] Zr(salphen)Cl$_2$,[9] FeCl$_3$,[2] and (NH$_4$)$_2$[Ce(NO$_3$)$_6$],[10] have produced the desired indolinones in good to excellent yields. A range of other acid catalysts such as *p*-toluenesulfonic acid,[11] sulfamic acid,[12] and Wells−Dawson-type tungstophosphoric heteropolyacid[13] have also been utilized to carry out the synthesis. However, most of the above methods are associated with one or more drawbacks, such as the use of exhaustible metal reserves, harsh and corrosive acids, tedious workup procedures, and unrecyclable catalysts. Therefore, various heterogeneous catalysts have been fabricated and successfully utilized;[14−19] nevertheless, their recyclability remains challenging due to cumbersome and time-consuming filtration and centrifugation procedures.
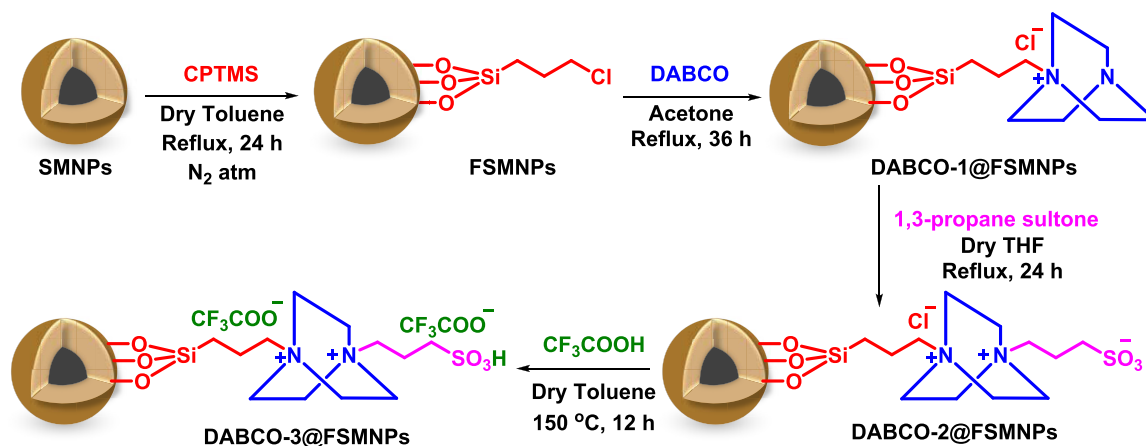
In this regard, ionic liquids (ILs) have emerged as green and recyclable alternatives to both conventional solvents and

Figure 1. Examples of biologically active 3,3-di(indolyl)indolin-2-ones.

Scheme 1. Schematic Illustration for the Synthesis of DABCO-3@FSMNPs

catalysts.[20,21] Since recent years, they have been involved in catalyzing reactions, explicitly through hydrogen-bonding interactions, which were classically catalyzed using metals and acids.[22,23] They possess low vapor pressures, high thermal and chemical stability, high ionic conductivity, and a large solubility window that can dissolve both organic and inorganic materials.[24,25] All of these features attribute green and environment-friendly credentials to organic reactions. In this context, scientists have greatly acknowledged their properties in the synthesis of 3,3-di(indolyl)indolin-2-ones. A variety of ILs such as imidazolium-based,[26] guanidinium-based,[27] and 1,4-diazabicyclo[2.2.2]octane (DABCO)-based[28−30] cations have served their role as catalysts in the reaction of isatin and indole. Although each and every catalytic system imparts good to excellent yields, they offer large scope for improvement due to associated drawbacks, including slow diffusion of substrates, tedious product isolation, troublesome IL recycling procedures, and their possible degradation during recycling.[31]

Thus, to enhance the catalytic efficiency and to make the catalytic recovery more facile, immobilization of ionic liquids has emerged as an ideal solution, which would combine the advantages of ILs and heterogeneous solid support materials.[32−34] For this, silica-coated magnetite nanoparticles (SMNPs) would be the ultimate choice for catalytic support due to their remarkable nanoscale dimensions leading to high surface area to volume ratio, magnetic recoverability, ease of functionalization, high thermal stability, and augmented dispersibility in polar reaction media. The silica coating over magnetite nanoparticles also provides resistance toward possible degradation and agglomeration, and thereby, confers chemical stability.[35−38]

Therefore, as part of our continuing efforts to develop green and sustainable nanocatalysts for various organic transformations,[35,39−47] herein, we report the design, fabrication, and characterization of a silica-coated magnetite-nanoparticle-supported DABCO-derived and acid-functionalized ionic liquid for the synthesis of bioactive 3,3-di(indolyl)indolin-2-ones. Among a variety of IL synthons, DABCO was selected for quaternization. It is a tertiary amine having sufficient alkalinity and medium hindrance that help in facile reactions with various groups. Its cagelike structure enhances the energy barrier of nitrogen inversion by 7 kcal mol^{-1} in comparison to trialkylamine.[48−50] This makes the lone pair of nitrogen more localized, which in turn increases its availability for the quaternization reaction. After the successful synthesis of the

supported IL, the nanocatalytic system utilizes green reaction medium, mild reaction conditions, and short reaction times to synthesize desired indolinones in good to excellent yields. In addition, the catalyst confers effortless magnetic recovery and excellent reusability, which contribute toward sustainability. To the best of our knowledge, this is the first report wherein an SMNP-supported acid-functionalized DABCO-based ionic liquid has been utilized for the synthesis of 3,3-di(indolyl)-indolin-2-ones.

■ RESULTS AND DISCUSSION

Preparation of the Catalyst. The synthesis of the catalyst was performed in five steps, as illustrated in Scheme 1. For the fabrication of the catalyst, SMNPs were chosen as the support material for immobilizing the required task-specific IL. Initially, SMNPs were reacted with CPTMS to provide a functionalization site. The obtained FSMNPs were further treated with DABCO to form the first precursor of the required IL. After the successful formation of DABCO-1@FSMNPs, functionalization was done with 1,3-propane sultone and trifluoroacetic acid to deliver acidic features to the final catalyst.

Characterization of the Catalyst. *Fourier Transform Infrared (FT-IR) Spectroscopic Analysis.* FT-IR spectroscopy was used to confirm the successful formation of the nanosupport and the grafting of the DABCO-based acid-functionalized ionic liquid on the surface of SMNPs (Figure 2). In all spectra, absorption bands near 3400−3500 cm^{-1} are attributed to the presence of surface hydroxyl groups. In Figure
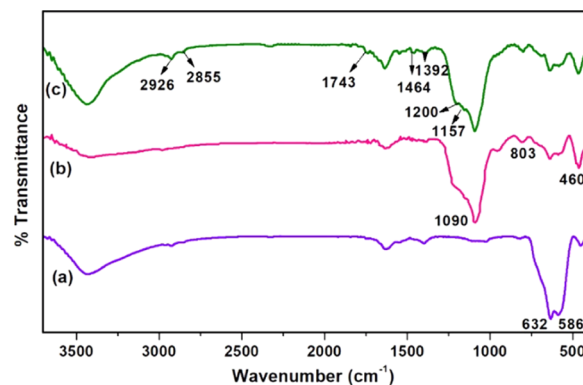

Figure 2. FT-IR spectra of (a) MNPs, (b) SMNPs, and (c) DABCO-3@FSMNPs.

2a, strong peaks at 632 and 586 cm^{-1} emerged due to Fe−O vibrations, which validate the synthesis of Fe$_3$O$_4$ nanoparticles.[51] The formation of the silica coating on MNPs is confirmed by the appearance of intense peaks at 1090, 803, and 460 cm^{-1}, which occurred due to the Si−O−Si stretching, Si−O bending, and Si−O−Si bending vibrations (Figure 2b).[52] In Figure 2c, only marginal changes can be seen with strong dominant bands of the nanosupport. The peaks at 2926 and 2855 cm^{-1} are ascribed to the C−H antisymmetric and symmetric stretching bands of the methylene group. Also, a weak peak at 1464 cm^{-1} appeared due to aliphatic CH$_2$ bending. The bonding of DABCO on SMNPs is confirmed by the emergence of C−N stretching peaks at 1157 and 1200 cm^{-1}.[53,54] An additional peak at 1392 cm^{-1} originates from the asymmetrical stretching of S=O bonds of −SO$_3$H groups.[55] Besides, the weak peak at 1743 cm^{-1} is assigned to the vibrational modes of the carbonyl group in trifluoroacetate. A difference in the position and intensity of the carbonyl peak is observed, which can be attributed to the existence of ionic interactions between the groups on the immobilized ionic liquid.[56]

X-ray Diffraction (XRD) Analysis. To determine the crystallographic properties, structure, and size of the synthesized nanomaterials, XRD analysis of MNPs, SMNPs, and DABCO-3@FSMNPs was performed (Figure 3). It was
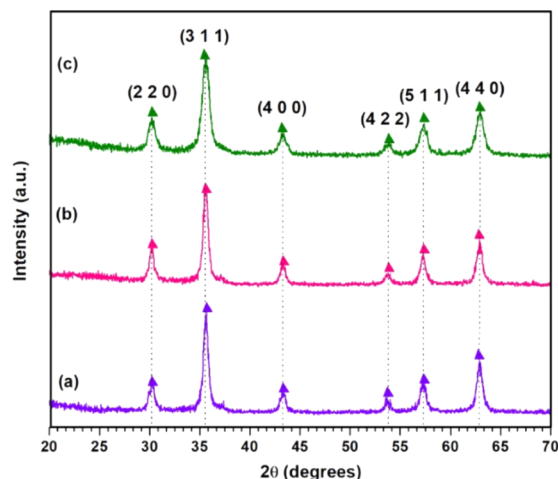
Figure 3. XRD spectra of (a) MNPs, (b) SMNPs, and (c) DABCO-3@FSMNPs.

observed that the position of all peaks in the XRD pattern of MNPs matched with that of the standard XRD pattern of the cubic inverse spinel structure of magnetite (Joint Committee

on Powder Diffraction Standards (JCPDS) card no. 19-0629). Figure 3a contains six strong Bragg's diffraction peaks at 2θ = 30.20, 35.53, 43.27, 53.80, 57.31, and 62.87°, corresponding to the (220), (311), (400), (422), (511), and (440) crystalline planes of the magnetite phase, respectively.[57] Furthermore, the above-mentioned peaks, with no additional peaks, were obtained in the XRD patterns of SMNPs and the catalyst, which prove retention of the magnetite structure in the nanoparticles even after surface modification. However, the presence of silica was not observed in the XRD spectra of SMNPs and the catalyst, implying its high dispersity over the nanocomposites.[58] XRD can also be used to estimate the crystallite size of particles using the Scherrer equation, according to which $D_{hkl} = k\lambda/\beta \cos\theta$, where D_{hkl} is the mean size of the crystalline domains in a direction perpendicular to the lattice plane, hkl are the Miller indices of the plane under consideration, k is a dimensionless shape factor (0.89 for spherical particles), λ is the X-ray wavelength (0.15418 nm for Cu Kα), β is the full line width at half-maximum intensity (FWHM; in radians), and θ is the Bragg angle (in degrees). As per this equation, the size of the magnetite nanoparticles was calculated, taking into account the diffraction peak with the maximum intensity, and was found to be approximately 11 nm.

Field-Emission Scanning Electron Microscopic (FE-SEM) Analysis. The surface morphology of the synthesized nanocomposites was studied using FE-SEM. Figure 4a demonstrates that the MNPs are uniform spheres, whose surface becomes rough and spongy after coating with silica (Figure 4b). The FE-SEM image of the final nanocatalyst also reveals that the morphology of the catalyst remains intact even after surface functionalization with various organic moieties (Figure 4c).

Transmission Electron Microscopic (TEM) Analysis. TEM analysis was done to gain insights into the size and structure of MNPs, SMNPs, and the final catalyst, DABCO-3@FSMNPs. Figure 5a unveils the nearly uniform and spherical nature of MNPs with an average diameter of 10.5 nm, which is in good accord with XRD results. SMNPs can be viewed as spherical core−shell nanoparticles with a dense magnetite core at the center and a uniformly dispersed amorphous silica coating at the boundary of MNPs (Figure 5b). The thickness of the silica shell was measured to be 4−5 nm. The electron micrograph of DABCO-3@FSMNPs reveals nearly similar structural features to those in Figure 5b, conveying that surface modification does not alter the morphology of SMNPs (Figure 5c). The size distribution diagrams of the nanosupport and the catalyst are provided in Figure S1, which show that the size of MNPs, SMNPs, and DABCO-3@FSMNPs is 10−10.5, 18−20, and 20−21 nm, respectively.
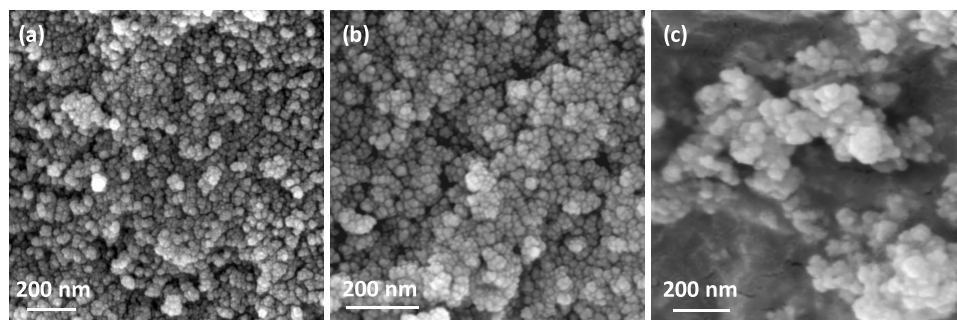
Figure 4. FE-SEM images of (a) MNPs, (b) SMNPs, and (c) DABCO-3@FSMNPs.
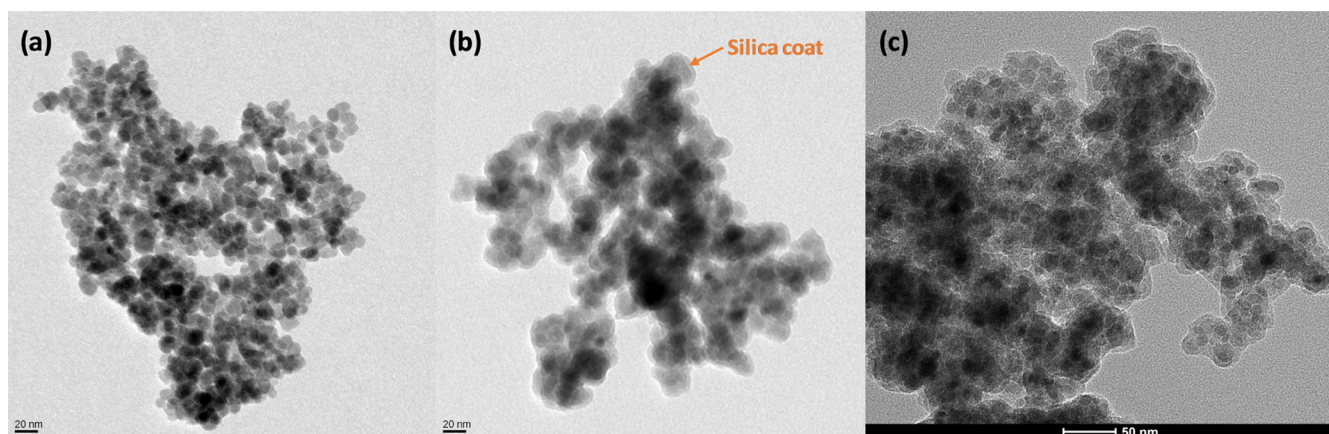
Figure 5. TEM images of (a) MNPs, (b) SMNPs, and (c) DABCO-3@FSMNPs.

Vibrating Sample Magnetometric (VSM) Analysis. The recyclability of a catalyst depends on its capability to be recovered. Magnetic nanocatalysts possess substantial features that are beneficial from the viewpoint of green chemistry, such as effortless and economic recovery, and thereby, sustainability. Consequently, the magnetic properties of the fabricated nanocomposites were examined using VSM at room temperature with a magnetic field varying from −10 000 to +10 000 Oe. Figure 6 illustrates that upon modification of MNPs with
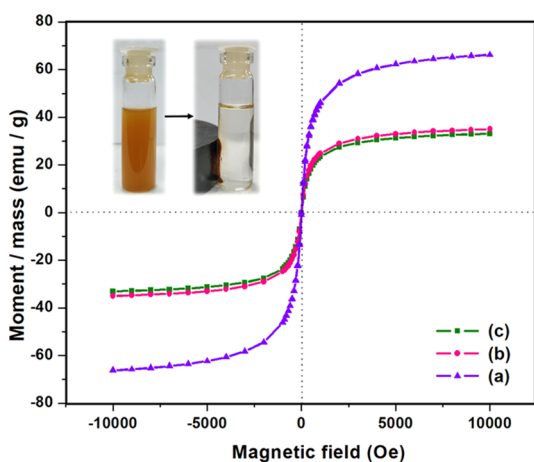

Figure 6. Magnetization curves of (a) MNPs, (b) SMNPs, and (c) DABCO-3@FSMNPs. Inset: facile separation of the catalyst using an external magnet.

diamagnetic silica and other organic moieties of the ionic liquid, the saturation magnetization value (M_s) decreases from MNPs (66.2 emu g^{-1}) to SMNPs (35 emu g^{-1}), and to the final catalyst (33 emu g^{-1}). In spite of the decrease in M_s values, the catalyst could be easily recovered from the reaction medium with the aid of an external magnet within a few seconds (Figure 6 inset). Besides, the magnetization curves depict the superparamagnetic nature of the synthesized nanoparticles, as no hysteresis loop, remanence, or coercivity was observed in any of the curves.

X-ray Photoelectron Spectroscopy (XPS). To acquire information about the chemical composition of DABCO-3@FSMNPs, XPS analysis was carried out (Figure 7a). In the high-resolution spectrum of Fe 2p, two peaks were observed at 725 and 711 eV, which were assigned to Fe 2p$_{1/2}$ and Fe 2p$_{3/2}$

of Fe$_3$O$_4$, respectively (Figure 7b).[59] Further, a peak at 104 eV was also seen, which confirmed the presence of the silica coating over MNPs (Figure 7c). Moreover, the contribution from carbon species was indicated by the peaks at 293 and 286 eV, which appeared due to CF$_3$ and C−C, C−O, and C=O, respectively (Figure 7d).[60] Also, two distinct peaks at 403 and 400 eV were observed in the N 1s region (Figure 7e).[61] In addition, the peaks at 533 and 690 eV were attributed to O 1s and F 1s, respectively (Figure 7f,g).[62] Besides, a peak at 169 eV was assigned to the binding energy for the S 2p electron of the −SO$_3$H group (Figure 7h).[63] The elemental composition was also verified by the presence of Fe, Si, N, O, F, and S in the energy dispersive X-ray analysis (EDAX) spectrum of DABCO-3@FSMNPs (Figure S2).

Thermogravimetric Analysis (TGA). The thermal stability of the as-synthesized nanomaterials was studied using TGA. As depicted in Figure 8a,b, the TGA curves of MNPs and SMNPs show no substantial weight loss. In Figure 8c, the initial weight loss (of about 4%) from room temperature to 280 °C is caused by the evaporation of adsorbed water and other organic solvents that were utilized during catalyst synthesis. As the temperature rises, the catalyst gets broken down in two steps; 280−400 and 400−580 °C due to the decomposition of organic species that were used for the formation and immobilization of the ionic liquid onto the support.[64,65] At higher temperatures, above 580 °C, only a slight weight loss is observed, which indicates the presence of remaining silica and Fe$_3$O$_4$ nanoparticles.

Catalytic Activity. The catalytic efficiency of the synthesized catalyst, DABCO-3@FSMNPs, was investigated in the formation of 3,3-di(indolyl)indolin-2-one derivatives via the pseudo-three-component one-pot reaction of indoles with isatins. After going through the literature reports, it was found that the reaction under consideration has been carried out in a variety of solvents or solvent mixtures, including CH$_2$Cl$_2$, CH$_3$CN, C$_2$H$_5$OH, CH$_3$OH, and H$_2$O. However, considering the impact of volatile-organic-compound-based solvents on human health and the environment, H$_2$O was chosen as the green solvent for further studies. This will also reduce the dependence on fossil fuels for obtaining carbon-based solvents.[66] To commence the investigation, indole and isatin were selected as the model substrates, which were reacted in the absence of the catalyst under aqueous conditions (Table 1, entries 1 and 2). When no product was detected even after 5 h, a catalytic amount of DABCO-3@FSMNPs was added (Table
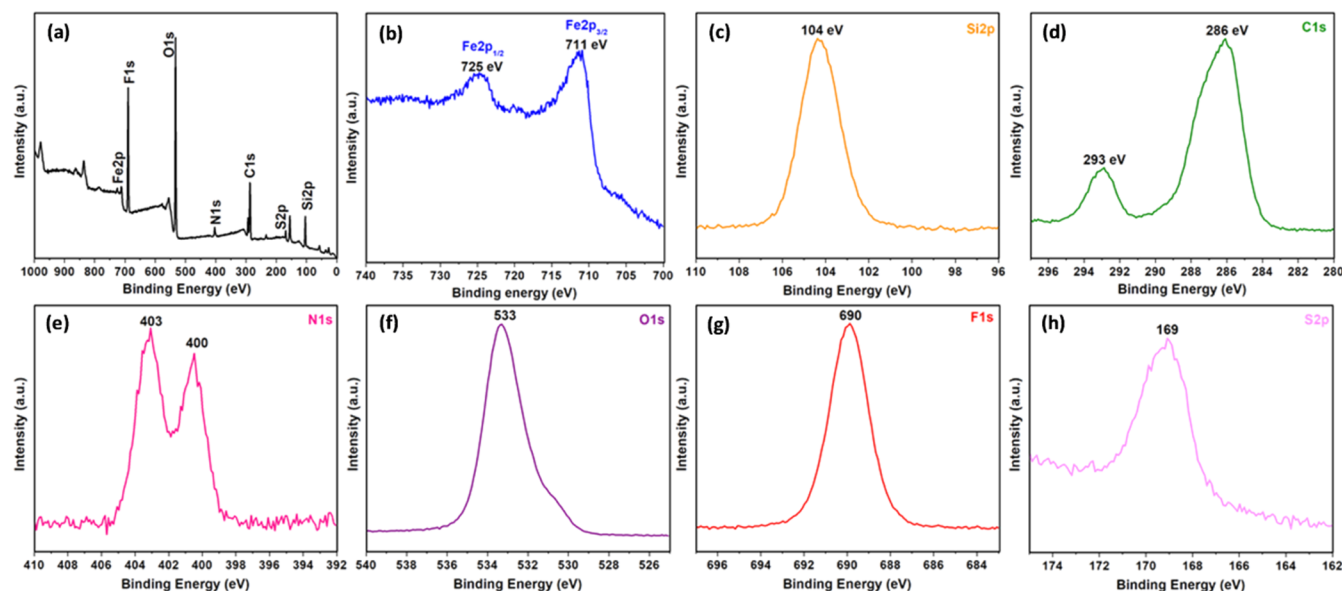
Figure 7. (a) XPS survey spectrum of DABCO-3@FSMNPs and detailed XPS spectra of (b) Fe 2p, (c) Si 2p, (d) C 1s, (e) N 1s, (f) O 1s, (g) F 1s, and (h) S 2p.
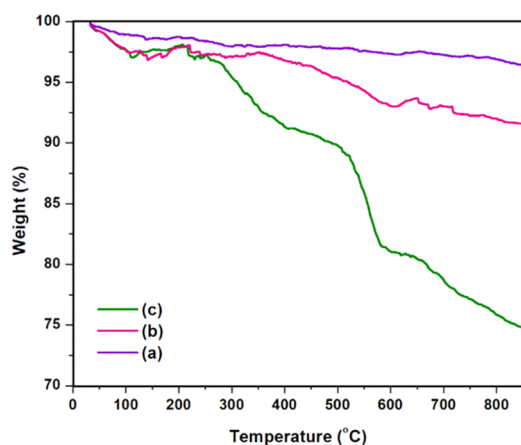

Figure 8. TGA curves of (a) MNPs, (b) SMNPs, and (c) the DABCO-3@FSMNP catalyst.

1, entries 3 and 4). The preliminary results were encouraging, as 96% of 3,3-di(indolyl)indolin-2-one was obtained as the sole product under refluxing conditions (Table 1, entry 4). Hence, to study the effect of temperature on product yield, the temperature of the reaction was lowered from 100 to 70 °C (Table 1, entries 4−6). Results indicated that 90 °C was the optimized temperature. To further improve the reaction conditions, the amount of catalyst was varied (Table 1, entries 7−9). It was observed that on lowering the catalytic amount to 50 mg, no substantial changes were observed; however, a further decrease was not in favor of the product yield. The best results were obtained with 50 mg of the catalyst. Finally, the effect of reaction time was monitored (Table 1, entries 10−12). To our delight, excellent yield of the desired product was obtained in just 2 h (Table 1, entry 11). The catalytic efficiencies of various precursor materials were also analyzed for the concerned reaction (Table S1). However, no significant product yield was observed in any of the cases, justifying the utility of the DABCO-based acidic ionic liquid for the efficient synthesis of 3,3-di(indolyl)indolin-2-one derivatives.

Table 1. Optimization of Reaction Conditions for the Synthesis of 3,3-Di(indolyl)indolin-2-ones[a]

S. No.	catalyst	amount of catalyst (mg)	temperature (°C)	time (h)	% yield[b]
1			RT	5	
2			100	5	trace
3	DABCO-3@FSMNPs	70	RT	5	trace
4	DABCO-3@FSMNPs	70	100	5	96
5	DABCO-3@FSMNPs	70	90	5	96
6	DABCO-3@FSMNPs	70	70	5	78
7	DABCO-3@FSMNPs	90	90	5	95
8	DABCO-3@FSMNPs	50	90	5	96
9	DABCO-3@FSMNPs	40	90	5	87
10	DABCO-3@FSMNPs	50	90	3	96
11	DABCO-3@FSMNPs	50	90	2	96
12	DABCO-3@FSMNPs	50	90	1	63

[a]Reaction conditions: Isatin (0.5 mmol), indole (1 mmol), H_2O (2 mL). [b]Isolated yields.

With the optimized conditions in hand, we expanded our attention toward a variety of indoles and isatins to synthesize a library of 3,3-di(indolyl)indolin-2-ones with 50 mg of the DABCO-3@FSMNP catalyst under aqueous conditions at 90 °C in 2 h (Table 2). All reactions proceeded smoothly yielding the desired products in good to excellent yields. Indoles having functional groups, such as bromo and methoxy, were reacted with isatins containing different halides (Table 2, entries 1-11). Remarkably, high product yields were obtained in each case. Even the nitro group was well tolerated under identical conditions (Table 2, entry 12). However, when 2-substituted indole was reacted with isatin, no product was detected, which

Table 2. Catalytic Efficacy of DABCO-3@FSMNPs in the Synthesis of Various 3,3-Di(indolyl)indolin-2-ones[a]

S. No.	Indole	Isatin	Yield (%)[b]
1.			96
2.			91
3.			98
4.			92
5.			89
6.			91
7.			89
8.			85
9.			88
10.			87
11.			89
12.			90
13.			-

[a]Reaction conditions: isatin (0.5 mmol), indole (1 mmol), DABCO-3@FSMNPs (50 mg), H_2O (2 mL), 90 °C, 2 h. [b]Isolated yields.

could be attributed to the presence of steric hindrance between two 2-substituted indoles in 3,3-di(indolyl)indolin-2-ones (Table 2, entry 13).

Proposed Reaction Mechanism. On the grounds of optimization results and previous reports, a plausible reaction mechanism has been proposed for the synthesis of 3,3-di(indolyl)indolin-2-ones using DABCO-3@FSMNPs as the catalytic entity. As depicted in Scheme 2, both cationic and anionic species of the immobilized ionic liquid (I) participate in the formation of hydrogen bonds with the reactants, indole and isatin, and hence, catalyze the reaction through a relay of

cooperative interactions (II).[67] Initially, the proton of the sulfonic acid functionality activates the carbonyl carbon of isatin by acting as an H-bond donor, thereby making the site more electrophilic.[28] Simultaneously, trifluoroacetate accepts an H-bond from the N—H of indole, and thus, facilitates the nucleophilic attack of indole via its C-3 carbon on the electron-deficient carbonyl carbon of activated isatin to generate species (III). Subsequently, after hydrogen transfer (IV), dehydration takes place to form an intermediate (V) where nucleophilic attack of another activated indole molecule leads to the formation of the targeted product and regenerates the catalyst.[12,30]

Catalyst Recyclability and Stability Test. Recyclability is one of the fundamental features of a catalyst that controls the economy and efficiency of a process at the industrial scale.[68] Hence, to measure the efficacy of our catalyst, catalytic recyclability studies were carried out using isatin and indole as the model substrates. After each cycle, the catalyst was separated from the reaction mixture, using a simple external magnet, washed with acetone, and dried under vacuum for its subsequent usage. Figure 9 testifies that the catalyst can be used for eight successive runs without any appreciable decrease in product yield. To scrutinize any physicochemical changes in the catalyst after recycling, various characterization techniques were employed (Figure S3). The FT-IR spectrum of the recovered catalyst shows no changes in the absorption peaks, which authenticate that the chemical stability of the catalyst is sustained. Also, FE-SEM and TEM images validate no morphological changes in the recycled catalyst. Moreover, there is no substantial change in the M_s values of the fresh and recovered catalysts.

Besides, to test the possible leaching of catalytic species, the reaction mixture was subjected to a split test. For this, during the reaction of indole and isatin, the catalyst was removed from the reaction mixture after 1 h. Afterward, the reaction medium was divided into two equal halves. One of the two parts was continued under the catalyst-deficit reaction conditions. After 4 h, the reaction was stopped, and the two reaction mixtures were analyzed to determine the product yield. Fortunately, identical yield of the desired product was achieved in both cases, which overruled leaching and strongly confirmed the truly heterogeneous nature of the catalyst. All of the above features contribute toward the large-scale applicability of DABCO-3@FSMNPs in various pharmaceutical applications.

Literature Precedents. To date, a variety of homogeneous metal catalysts, acids, and ionic liquids have been utilized for the successful formation of 3,3-di(indolyl)indolin-2-ones. Besides, various supported acid catalysts and metal complexes have also furnished the desired products in good yields. Table 3 outlines a brief summary of the literature reports to compare the catalytic efficiency of DABCO-3@FSMNPs with that obtained in previously reported methodologies. To our delight, the present catalyst utilizes comparable reaction conditions and proves its supremacy in terms of effortless magnetic recoverability and reusability up to eight cycles.

■ CONCLUSIONS

In conclusion, we have successfully fabricated and characterized a silica-coated magnetic-nanoparticle-supported acid-functionalized DABCO-based ionic liquid. The as-synthesized nanocomposite showed remarkable catalytic efficacy in the synthesis of various bioactive 3,3-di(indolyl)indolin-2-ones in good to excellent yields. Some of the admirable features of the

Scheme 2. Plausible Reaction Mechanism for the Synthesis of 3,3-Di(indolyl)indolin-2-ones Using DABCO-3@FSMNPs
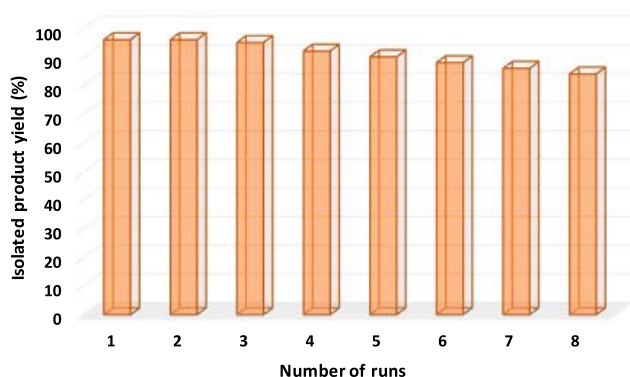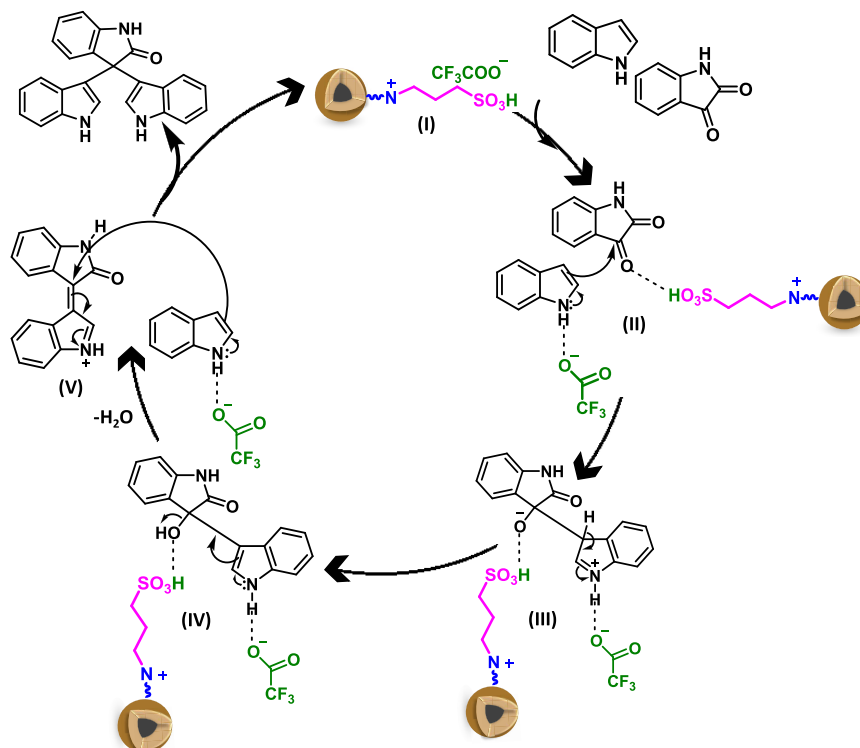

Figure 9. Recyclability test for the synthesis of 3,3-di(indolyl)indolin-2-ones using DABCO-3@FSMNPs. Reaction conditions: isatin (0.5 mmol), indole (1 mmol), recovered catalyst, H_2O (2 mL), 90 °C, 2 h.

current catalytic system include utilization of mild and ecofriendly reaction conditions, broad substrate scope, and requirement of only a catalytic amount of the immobilized IL. Also, when compared with the previously reported protocols, DABCO-3@FSMNPs turned out to be a better catalytic entity in terms of effortless magnetic recoverability and reusability up to eight consecutive cycles without any significant compromise in either catalytic efficiency or physicochemical properties. All of these features offer noncompetitive opportunities for the use of DABCO-3@FSMNPs at a large industrial scale.

■ **EXPERIMENTAL SECTION**

Materials and Reagents. Most of the chemicals were commercially available and used without further purification. Ferric sulfate hydrate and ferrous sulfate heptahydrate were purchased from Fischer Scientific. Tetraethyl orthosilicate (TEOS) and (3-chloropropyl)trimethoxysilane (CPTMS)

were procured from Sigma Aldrich. 1,4-Diazabicyclo[2.2.2]-octane (DABCO) and 1,3-propane sultone were obtained from Alfa Aesar. Trifluoroacetic acid was acquired from Sisco Research Laboratories Pvt. Ltd. All other reagents and organic compounds were of analytical grade and purchased from Alfa Aesar and Thomas Baker Chemicals. Besides, double-distilled water was used throughout the experiments.

Characterization Techniques. The as-synthesized nano-composites were thoroughly characterized using various physicochemical techniques to gain insights into the composition, morphology, functionality, crystallinity, stability, and other important characteristics. Fourier transform infrared spectroscopic studies were carried out on a PerkinElmer Spectrum 2000 using the KBr pellet method in a scanning range of 4000−400 cm^{-1}. X-ray diffractograms were acquired on a Rigaku MiniFlex in the 2θ range of 20−70° at a scan rate of 2° min^{-1}. Field-emission scanning electron micrographs were collected using a Tescan LYRA 3 FE-SEM microscope. Prior to sample preparation, clean metal stubs were glued with an adhesive, such as conductive double-sided carbon tape in our case. Furthermore, finely crushed and dried powdered nanoparticles were mounted onto the stubs followed by coating with gold to make them conductive using a Quorum Q150RS sputter coater. Transmission electron microscopy images were acquired on a FEI TECNAI G^2 T20 and Talos cryo TEM instrument. TEM samples were prepared by casting a drop of dispersed nanoparticles, in ethanol, on carbon-coated copper grids. ImageJ software was used for determination of size of nanoparticles using TEM images. An AMETEK EDAX system and a K-Alpha X-ray photoelectron spectrometer were used to analyze the elemental composition of the supported ionic liquid. Magnetization values of the nanocomposites were measured on a MicroSense ADE-EV9 at room temperature between −10 000 and +10 000 Oe. Thermogravimetric curves were acquired using a Linseis TGA under a nitrogen

Table 3. Comparison of the Catalytic Activity of the DABCO-3@FSMNP Nanocatalyst with That of Literature Precedents

S. No.	catalyst	reaction conditions	yield (%)[a]	recyclability	reference
1	Bi(OTf)$_3$ (2 mol %)	CH$_3$CN, RT, 3 h	92		7
2	Zn(OTf)$_2$ (1 mol %)	CH$_3$CN, RT, 5 min	94		8
3	Zr(salphen)Cl$_2$ (1 mol %)	EtOH, RT, 25 min	85		9
4	FeCl$_3$ (5 mol %)	CH$_3$CN, RT, 15 min	93		2
5	ceric ammonium nitrate (10 mol %)	anhydrous EtOH, ultrasonication, 3 h	95		10
6	p-TSA (10 mol %)	CH$_2$Cl$_2$, RT, 20 min	92		11
7	silica-gel-supported In(acac)$_3$ (10 wt %)	H$_2$O/CH$_3$CN, RT, 2.5 h	92	6 cycles	14
8	nano-NiO (4 mg)	H$_2$O, 70 °C, 0.5 h	98	5 cycles	19
9	amberlyst 15 (0.3 g)	H$_2$O, 70 °C, 0.5 h	94	3 cycles	15
10	β-cyclodextrin−SO$_3$H (10 mol %)	H$_2$O, 100 °C, 5 min	96	4 cycles	18
11	sulfamic acid (20 mol %)	EtOH/H$_2$O, RT, 2 h	89	3 cycles	12
12	H$_6$P$_2$W$_{18}$O$_{62}$ (5 mol %)	H$_2$O, 60 °C, 30 min	95	3 cycles	13
13	nano-SiO$_2$-BF$_3^-$CH$_3$OH$_2^+$ (300 mg)	CH$_3$OH, reflux, 0.33 h	95	5 cycles	69
14	[Dabco-C$_2$OH][FeCl$_4$] (10 mol %)	EtOH, 50 °C, 15 min	98	6 cycles	30
15	[Dabco-H][HSO$_4$] (10 mol %)	H$_2$O, 90 °C, 2 h	96	6 cycles	28
16	N,N,N,N-tetramethyl guanidinium trifluoroacetate (TMGT) (1 mL)	RT, 1 h	93		27
17	(i) [Dabco-H][BF$_4$] (10 mol %)	(i) H$_2$O, 55 °C, 1 h	(i) 85	6 cycles	29
	(ii) [Dabco-H][HSO$_4$] (10 mol %)	(ii) H$_2$O, 90 °C, 0.5 h	(ii) 98		
18	Fe$_3$O$_4$−OSO$_3$H	EtOH, reflux, 3 h	92		70
19	DABCO-3@FSMNPs (50 mg)	H$_2$O, 90 °C, 2 h	96	8 cycles	present work

[a]Isolated yields.

atmosphere with a gas flow of 2 L h^{-1} and in the range of room temperature to 850 °C at a heating rate of 10 °C min^{-1}. Finally, the synthesized organic compounds were characterized using a ^{1}H (400 MHz) and ^{13}C (100 MHz) JEOL JNM-EXCP-400 nuclear magnetic resonance spectrophotometer. Spectra were recorded in DMSO-d_6. Chemical shifts (δ) for proton and carbon are reported in parts per million (ppm) units downfield from tetramethylsilane (internal standard) and data are documented as chemical shift (multiplicity, coupling constant, integration).

Catalyst Preparation. *Synthesis of the Nanosupport (SMNPs).* Considering the benefits of magnetically separable catalysts, silica-coated magnetic nanoparticles (SMNPs) were chosen as the catalytic support. Magnetite nanoparticles (MNPs) were synthesized using the coprecipitation technique.[71] Initially, 6.0 g (15 mmol) of ferric sulfate hydrate and 4.2 g (15 mmol) of ferrous sulfate heptahydrate were dissolved in a round-bottom flask containing 250 mL of double-distilled water. The above solution was stirred at 60 °C until the solution turned yellowish-orange. Next, 15 mL of aqueous ammonia (25%) was added into the above solution to adjust the pH to 10. After stirring for an additional 30 minutes, the black precipitate obtained was separated using an external magnet, washed several times with double-distilled water (until the pH turned neutral), and dried in a vacuum oven. To obtain a silica coating over MNPs, the sol−gel method was adopted.[72] For this, 0.5 g of MNPs were activated in 2.2 mL of 0.1 M HCl solution. Furthermore, the activated MNPs were dispersed in a 250 mL mixture of ethanol and double-distilled water (4:1) in an ultrasonic bath. Next, 5 mL of aqueous ammonia (25%) and 1 mL of TEOS was added dropwise during sonication. The solution was then stirred at 60 °C for 6 h. The resultant brownish precipitate was separated magnetically, washed with water and ethanol until neutral conditions, and finally dried in a vacuum oven to obtain amorphous SMNPs.

Functionalization of SMNPs (FSMNPs). The as-synthesized SMNPs were functionalized with CPTMS. The synthesis was carried out using 1.0 g of dispersed SMNPs in 100 mL of dry toluene and adding 20 mmol of CPTMS under reflux conditions in a nitrogen atmosphere for 24 h. The solid obtained was separated magnetically, washed with diethyl ether, and dried in a vacuum oven to obtain FSMNPs.

Surface Modification of FSMNPs. FSMNPs were surface modified to obtain the DABCO-based ionic liquid. FSMNPs (1.0 g) were dispersed in 100 mL of acetone under ultrasonication. Furthermore, 20 mmol of DABCO was added to the above solution and refluxed under air for 36 h. The so-formed solid was magnetically separated, washed several times with acetone, and dried in a vacuum oven to obtain DABCO-1@FSMNPs. These nanoparticles were further modified to quaternize the other nitrogen. For this, 1.0 g of DABCO-1@FSMNPs were dispersed in 100 mL of dry tetrahydrofuran (THF) under ultrasonication, followed by addition of 20 mmol 1,3-propane sultone and further refluxing for 24 h. The obtained DABCO-2@FSMNPs were magnetically separated, washed with THF and ethanol, and dried in a vacuum oven.

Acid Functionalization of FSMNPs (DABCO-3@FSMNPs). Lastly, to obtain silica-coated magnetic-nanoparticle-supported DABCO-based acidic ionic liquid, 1.0 g of DABCO-2@FSMNPs were dispersed in 50 mL of dry toluene. Further, 20 mmol trifluoroacetic acid was added dropwise into the dispersed solution. After the addition was completed, the solution was heated at 150 °C for 12 h. The final nanocatalyst, DABCO-3@FSMNPs, was magnetically separated, washed with diethyl ether, and dried in a vacuum oven.

General Reaction Procedure for the Synthesis of 3,3-Di(indolyl)indolin-2-ones. The synthesis of 3,3-di(indolyl)-indolin-2-ones involves the reaction of indoles and isatins. For the reaction, 1 mmol indole and 0.5 mmol isatin were mixed in a 10 mL round-bottom flask containing 2 mL of distilled water. Further, DABCO-3@FSMNPs were added and heated in an oil bath at the specified temperature under constant stirring. The progress of the reaction was monitored by TLC. After the

completion of the reaction, a small amount of acetone was added and the catalyst was effortlessly separated from the vessel using an external magnet. The solvent was evaporated under reduced pressure, and the crude product was further subjected to column chromatography with silica gel as the stationary phase and methanol/dichloromethane (2:98) as the eluent.

■ ASSOCIATED CONTENT

Ⓢ Supporting Information

The Supporting Information is available free of charge at https://pubs.acs.org/doi/10.1021/acsomega.9b03237.

> Size distribution diagrams, EDAX spectrum of the catalyst, characterization of the recovered catalyst, catalytic efficiencies of various precursor materials for the synthesis of 3,3-di(indolyl)indolin-2-one, and ^{1}H and ^{13}C NMR spectra of isolated products (PDF)

■ AUTHOR INFORMATION

Corresponding Author
*E-mail: rksharmagreenchem@hotmail.com.

ORCID Ⓞ
Radhika Gupta: 0000-0002-2305-4867
Rakesh K. Sharma: 0000-0003-4281-876X

Notes
The authors declare no competing financial interest.

■ ACKNOWLEDGMENTS

■ REFERENCES

(1) Paira, P.; Hazra, A.; Kumar, S.; Paira, R.; Sahu, K. B.; Naskar, S.; Mondal, S.; Maity, A.; Banerjee, S.; Mondal, N. B.; Saha, P. Efficient synthesis of 3,3-diheteroaromatic oxindole analogues and their in vitro evaluation for spermicidal potential. *Bioorg. Med. Chem. Lett.* **2009**, *19*, 4786−4789.

(2) Kamal, A.; Srikanth, Y.; Khan, M. N. A.; Shaik, T. B.; Ashraf, M. Synthesis of 3,3-diindolyl oxindoles efficiently catalysed by FeCl₃ and their in vitro evaluation for anticancer activity. *Bioorg. Med. Chem. Lett.* **2010**, *20*, 5229−5231.

(3) Reddy, B. V. S.; Rajeswari, N.; Sarangapani, M.; Prashanthi, Y.; Ganji, R. J.; Addlagatta, A. Iodine-catalyzed condensation of isatin with indoles: a facile synthesis of di(indolyl)indolin-2-ones and evaluation of their cytotoxicity. *Bioorg. Med. Chem. Lett.* **2012**, *22*, 2460−2463.

(4) Wang, G.; Wang, J.; Xie, Z.; Chen, M.; Li, L.; Peng, Y.; Chen, S.; Li, W.; Deng, B. Discovery of 3,3-di (indolyl) indolin-2-one as a novel scaffold for α-glucosidase inhibitors: in silico studies and SAR predictions. *Bioorg. Chem.* **2017**, *72*, 228−233.

(5) Annuur, R. M.; Titisari, D. A.; Dinarlita, R. R.; Fadlan, A.; Ersam, T.; Nuryastuti, T.; Santoso, M. In *Synthesis and Anti-tuberculosis activity of Trisindolines*, AIP Conference Proceedings; AIP Publishing, 2018; p020088.

(6) Yoo, M.; Choi, S.-U.; Choi, K. Y.; Yon, G. H.; Chae, J.-C.; Kim, D.; Zylstra, G. J.; Kim, E. Trisindoline synthesis and anticancer activity. *Biochem. Biophys. Res. Commun.* **2008**, *376*, 96−99.

(7) Yadav, J. S.; SubbaReddy, B. V.; Gayathri, K. U.; Meraj, S.; Prasad, A. R. Bismuth (III) triflate catalyzed condensation of isatin with indoles and pyrroles: a facile synthesis of 3,3-diindolyl-and 3,3-dipyrrolyl oxindoles. *Synthesis* **2006**, *24*, 4121−4123.

(8) Praveen, C.; Narendiran, S.; Dheenkumar, P.; Perumal, P. Zn(OTf)₂-catalysed indolylation and pyrrolylation of isatins: efficient synthesis and biochemical assay of 3,3-di (heteroaryl) oxindoles. *J. Chem. Sci.* **2013**, *125*, 1543−1553.

(9) Jafarpour, M.; Rezaeifard, A.; Gorzin, G. Enhanced catalytic activity of Zr (IV) complex with simple tetradentate Schiff base ligand in the clean synthesis of indole derivatives. *Inorg. Chem. Commun.* **2011**, *14*, 1732−1736.

(10) Wang, S.-Y.; Ji, S.-J. Facile synthesis of 3,3-di(heteroaryl)-indolin-2-one derivatives catalyzed by ceric ammonium nitrate (CAN) under ultrasound irradiation. *Tetrahedron* **2006**, *62*, 1527−1535.

(11) Yu, J.; Shen, T.; Lin, Y.; Zhou, Y.; Song, Q. Rapid and efficient synthesis of 3,3-di (1H-indol-3-yl)indolin-2-ones and 2,2-di(1H-indol-3-yl)-2H-acenaphthen-1-ones catalyzed by p-TSA. *Synth. Commun.* **2014**, *44*, 2029−2036.

(12) Brahmachari, G.; Banerjee, B. Facile and one-pot access of 3,3-bis(indol-3-yl)indolin-2-ones and 2,2-bis(indol-3-yl)acenaphthylen-1(2H)-one derivatives via an eco-friendly pseudo-multicomponent reaction at room temperature using sulfamic acid as an organo-catalyst. *ACS Sustainable Chem. Eng.* **2014**, *2*, 2802−2812.

(13) Alimohammadi, K.; Sarrafi, Y.; Tajbakhsh, M. H₆P₂W₁₈O₆₂: A green and reusable catalyst for the synthesis of 3,3-diaryloxindole derivatives in water. *Monatsh. Chem.* **2008**, *139*, 1037−1039.

(14) Sharma, R. K.; Sharma, C. A highly efficient synthesis of oxindoles using a functionalized silica gel as support for indium (III) acetylacetonate catalyst in an aqueous-acetonitrile medium. *J. Mol. Catal. A: Chem.* **2010**, *332*, 53−58.

(15) Sarrafi, Y.; Alimohammadi, K.; Sadatshahabi, M.; Norozipoor, N. An improved catalytic method for the synthesis of 3,3-di(indolyl)oxindoles using Amberlyst 15 as a heterogeneous and reusable catalyst in water. *Monatsh. Chem.* **2012**, *143*, 1519−1522.

(16) Alinezhad, H.; Haghighi, A. H.; Salehian, F. A green method for the synthesis of bis-indolylmethanes and 3,3′-indolyloxindole derivatives using cellulose sulfuric acid under solvent-free conditions. *Chin. Chem. Lett.* **2010**, *21*, 183−186.

(17) Azizian, J.; Mohammadi, A. A.; Karimi, N.; Mohammadizadeh, M. R.; Karimi, A. R. Silica sulfuric acid a novel and heterogeneous catalyst for the synthesis of some new oxindole derivatives. *Catal. Commun.* **2006**, *7*, 752−755.

(18) Tayade, Y. A.; Patil, D. R.; Wagh, Y. B.; Jangle, A. D.; Dalal, D. S. An efficient synthesis of 3-indolyl-3-hydroxy oxindoles and 3,3-di(indolyl)indolin-2-ones catalyzed by sulfonated β-CD as a supra-molecular catalyst in water. *Tetrahedron Lett.* **2015**, *56*, 666−673.

(19) Nasseri, M. A.; Ahrari, F.; Zakerinasab, B. Nickel oxide nanoparticles: A green and recyclable catalytic system for the synthesis of diindolyloxindole derivatives in aqueous medium. *RSC Adv.* **2015**, *5*, 13901−13905.

(20) Welton, T. Room-temperature ionic liquids. Solvents for synthesis and catalysis. *Chem. Rev.* **1999**, *99*, 2071−2084.

(21) Cole, A. C.; Jensen, J. L.; Ntai, I.; Tran, K. L. T.; Weaver, K. J.; Forbes, D. C.; Davis, J. H. Novel Brønsted acidic ionic liquids and their use as dual solvent-catalysts. *J. Am. Chem. Soc.* **2002**, *124*, 5962−5963.

(22) Dong, K.; Zhang, S.; Wang, D.; Yao, X. Hydrogen bonds in imidazolium ionic liquids. *J. Phys. Chem. A* **2006**, *110*, 9775−9782.

(23) Zhang, L.; Fu, X.; Gao, G. Anion-cation cooperative catalysis by ionic liquids. *ChemCatChem* **2011**, *3*, 1359−1364.

(24) Amarasekara, A. S. Acidic ionic liquids. *Chem. Rev.* **2016**, *116*, 6133−6183.

(25) Vafaeezadeh, M.; Alinezhad, H. Brønsted acidic ionic liquids: green catalysts for essential organic reactions. *J. Mol. Liq.* **2016**, *218*, 95−105.

(26) Karimi, N.; Oskooi, H.; Heravi, M.; Saeedi, M.; Zakeri, M.; Tavakoli, N. On water: Brønsted acidic ionic liquid [(CH₂)₄SO₃HMIM][HSO₄] catalysed synthesis of oxindoles derivatives. *Chin. J. Chem.* **2011**, *29*, 321−323.

(27) Rad-Moghadam, K.; Sharifi-Kiasaraie, M.; Taheri-Amlashi, H. Synthesis of symmetrical and unsymmetrical 3,3-di(indolyl)indolin-2-ones under controlled catalysis of ionic liquids. *Tetrahedron* **2010**, *66*, 2316−2321.

(28) Tong, J.; Li, Y. W.; Xu, D. Z. Solvent-controlled Friedel-Crafts reaction for the synthesis of 3-indolyl-3-hydroxy oxindoles and 3,3-diindolyl oxindoles catalyzed by Dabco-base ionic liquids. *ChemistrySelect* **2017**, *2*, 3799−3803.

(29) Tong, J.; Huang, L.-S.; Xu, D.-Z. An efficient Friedel-Crafts alkylation for the synthesis of 3-indolyl-3-hydroxy oxindoles and unsymmetrical 3,3-diaryl oxindoles catalyzed by Dabco-based ionic liquids in water. *New J. Chem.* **2017**, *41*, 3966−3974.

(30) Gu, Y. C.; Hu, R. M.; Li, M. M.; Xu, D. Z. Iron-containing ionic liquid as an efficient and recyclable catalyst for the synthesis of C3-substituted indole derivatives. *Appl. Organomet. Chem.* **2019**, *33*, No. e4782.

(31) Wang, B.; Elageed, E. H.; Zhang, D.; Yang, S.; Wu, S.; Zhang, G.; Gao, G. One-pot conversion of carbon dioxide, ethylene oxide, and amines to 3-aryl-2-oxazolidinones catalyzed with binary ionic liquids. *ChemCatChem* **2014**, *6*, 278−283.

(32) Li, H.; Bhadury, P. S.; Song, B.; Yang, S. Immobilized functional ionic liquids: efficient, green, and reusable catalysts. *RSC Adv.* **2012**, *2*, 12525−12551.

(33) Valkenberg, M.; DeCastro, C.; Hölderich, W. Immobilisation of ionic liquids on solid supports. *Green Chem.* **2002**, *4*, 88−93.

(34) Mehnert, C. P. Supported ionic liquid catalysis. *Chem. - Eur. J.* **2005**, *11*, 50−56.

(35) Gupta, R.; Yadav, M.; Gaur, R.; Arora, G.; Sharma, R. K. A straightforward one-pot synthesis of bioactive *N*-aryl oxazolidin-2-ones *via* a highly efficient $Fe_3O_4@SiO_2$-supported acetate-based butylimidazolium ionic liquid nanocatalyst under metal-and solvent-free conditions. *Green Chem.* **2017**, *19*, 3801−3812.

(36) Gawande, M. B.; Monga, Y.; Zboril, R.; Sharma, R. K. Silica-decorated magnetic nanocomposites for catalytic applications. *Coord. Chem. Rev.* **2015**, *288*, 118−143.

(37) Sharma, R. K.; Yadav, M.; Gawande, M. B. Silica-coated magnetic nano-particles: application in catalysis. In *Ferrites and Ferrates: Chemistry and Applications in Sustainable Energy and Environmental Remediation*; ACS Publications, 2016; pp 1−38.

(38) Sharma, R. K.; Dutta, S.; Sharma, S.; Zboril, R.; Varma, R. S.; Gawande, M. B. Fe_3O_4 (iron oxide)-supported nanocatalysts: synthesis, characterization and applications in coupling reactions. *Green Chem.* **2016**, *18*, 3184−3209.

(39) Rana, P.; Gaur, R.; Gupta, R.; Arora, G.; Anireddy, J.; Sharma, R. K. Cross-dehydrogenative $C(sp^3)$-$C(sp^3)$ coupling *via* C-H activation using magnetically retrievable ruthenium-based photoredox nanocatalyst under aerobic conditions. *Chem. Commun.* **2019**, *55*, 7402−7405.

(40) Sharma, R. K.; Yadav, S.; Sharma, S.; Dutta, S.; Sharma, A. Expanding the horizon of multicomponent oxidative coupling reaction via the design of a unique, 3D copper isophthalate MOF-based catalyst decorated with mixed spinel $CoFe_2O_4$ nanoparticles. *ACS Omega* **2018**, *3*, 15100−15111.

(41) Sharma, R. K.; Sharma, A.; Sharma, S.; Dutta, S. Unprecedented ester-amide exchange reaction using highly versatile two-dimensional graphene oxide supported base metal nanocatalyst. *Ind. Eng. Chem. Res.* **2018**, *57*, 3617−3627.

(42) Sharma, R. K.; Gaur, R.; Yadav, M.; Goswami, A.; Zbořil, R.; Gawande, M. B. An efficient copper-based magnetic nanocatalyst for the fixation of carbon dioxide at atmospheric pressure. *Sci. Rep.* **2018**, *8*, No. 1901.

(43) Gaur, R.; Yadav, M.; Gupta, R.; Arora, G.; Rana, P.; Sharma, R. K. Aerobic oxidation of thiols to disulfides by silver-based magnetic catalyst. *ChemistrySelect* **2018**, *3*, 2502−2508.

(44) Arora, G.; Yadav, M.; Gaur, R.; Gupta, R.; Sharma, R. K. A novel and template-free synthesis of multifunctional double-shelled Fe_3O_4-C nanoreactor as an ideal support for confined catalytic reactions. *ChemistrySelect* **2017**, *2*, 10871−10879.

(45) Sharma, R. K.; Yadav, M.; Gaur, R.; Gupta, R.; Adholeya, A.; Gawande, M. B. Synthesis of iron oxide palladium nanoparticles and their catalytic applications for direct coupling of acyl chlorides with alkynes. *ChemPlusChem* **2016**, *81*, 1312−1319.

(46) Sharma, R. K.; Yadav, M.; Monga, Y.; Gaur, R.; Adholeya, A.; Zboril, R.; Varma, R. S.; Gawande, M. B. Silica-based magnetic manganese nanocatalyst-applications in the oxidation of organic halides and alcohols. *ACS Sustainable Chem. Eng.* **2016**, *4*, 1123−1130.

(47) Sharma, R. K.; Monga, Y.; Puri, A.; Gaba, G. Magnetite (Fe_3O_4) silica based organic-inorganic hybrid copper (II) nanocatalyst: a platform for aerobic *N*-alkylation of amines. *Green Chem.* **2013**, *15*, 2800−2809.

(48) Jamasbi, N.; Irankhah-Khanghah, M.; Shirini, F.; Tajik, H.; Langarudi, M. DABCO-based ionic liquids: introduction of two metal-free catalysts for one-pot synthesis of 1,2,4-triazolo [4,3-a] pyrimidines and pyrido [2,3-d] pyrimidines. *New J. Chem.* **2018**, *42*, 9016−9027.

(49) Ying, A.; Li, Z.; Yang, J.; Liu, S.; Xu, S.; Yan, H.; Wu, C. DABCO-based ionic liquids: recyclable catalysts for aza-Michael addition of *α*, *β*-unsaturated amides under solvent-free conditions. *J. Org. Chem.* **2014**, *79*, 6510−6516.

(50) Ying, A.; Ni, Y.; Xu, S.; Liu, S.; Yang, J.; Li, R. Novel DABCO based ionic liquids: green and efficient catalysts with dual catalytic roles for aqueous Knoevenagel condensation. *Ind. Eng. Chem. Res.* **2014**, *53*, 5678−5682.

(51) Zhang, J. L.; Srivastava, R.; Misra, R. Core-shell magnetite nanoparticles surface encapsulated with smart stimuli-responsive polymer: synthesis, characterization, and LCST of viable drug-targeting delivery system. *Langmuir* **2007**, *23*, 6342−6351.

(52) Lien, Y.-H.; Wu, T.-M. Preparation and characterization of thermosensitive polymers grafted onto silica-coated iron oxide nanoparticles. *J. Colloid Interface Sci.* **2008**, *326*, 517−521.

(53) Daragahi, S. A. H.; Mohebat, R.; Mosslemin, M. H. Green and eco-friendly synthesis of quinoxalines by Brönsted acidic ionic liquid supported on nano-SiO_2 under solvent-free conditions. *Org. Prep. Proced. Int.* **2018**, *50*, 301−313.

(54) Ying, A.; Liu, S.; Ni, Y.; Qiu, F.; Xu, S.; Tang, W. Ionic tagged DABCO grafted on magnetic nanoparticles: a water-compatible catalyst for the aqueous aza-Michael addition of amines to *α*, *β*-unsaturated amides. *Catal. Sci. Technol.* **2014**, *4*, 2115−2125.

(55) Kumar, V.; Nandy, A.; Das, S.; Salahuddin, M.; Kundu, P. P. Performance assessment of partially sulfonated PVdF-co-HFP as polymer electrolyte membranes in single chambered microbial fuel cells. *Appl. Energy* **2015**, *137*, 310−321.

(56) Jafarzadeh, M.; Soleimani, E.; Norouzi, P.; Adnan, R.; Sepahvand, H. Preparation of trifluoroacetic acid-immobilized $Fe_3O_4@SiO_2$-APTES nanocatalyst for synthesis of quinolines. *J. Fluorine Chem.* **2015**, *178*, 219−224.

(57) Abu-Reziq, R.; Alper, H.; Wang, D.; Post, M. L. Metal supported on dendronized magnetic nanoparticles: highly selective hydroformylation catalysts. *J. Am. Chem. Soc.* **2006**, *128*, 5279−5282.

(58) Baig, R. B. N.; Varma, R. S. A facile one-pot synthesis of ruthenium hydroxide nanoparticles on magnetic silica: aqueous hydration of nitriles to amides. *Chem. Commun.* **2012**, *48*, 6220−6222.

(59) Xiong, Z.; Li, S.; Xia, Y. Highly stable water-soluble magnetic nanoparticles synthesized through combined co-precipitation, surface-modification, and decomposition of a hybrid hydrogel. *New J. Chem.* **2016**, *40*, 9951−9957.

(60) Zhao, F.-G.; Zhao, G.; Liu, X.-H.; Ge, C.-W.; Wang, J.-T.; Li, B.-L.; Wang, Q.-G.; Li, W.-S.; Chen, Q.-Y. Fluorinated graphene: facile solution preparation and tailorable properties by fluorine-content tuning. *J. Mater. Chem. A* **2014**, *2*, 8782−8789.

(61) Mathew, R. T.; Cooney, R. P.; Malmstrom, J.; Doyle, C. S. Atomic force microscopy and angular-dependent X-ray photoelectron spectroscopy studies of anchored quaternary ammonium salt biocides on quartz surfaces. *Langmuir* **2018**, *34*, 4750−4761.

(62) Ebnesajjad, S.; Ebnesajjad, C. *Surface Treatment of Materials for Adhesive Bonding*; William Andrew, 2013.

(63) Varadwaj, G. B. B.; Rana, S.; Parida, K.; Nayak, B. B. A multi-functionalized montmorillonite for co-operative catalysis in one-pot Henry reaction and water pollution remediation. *J. Mater. Chem. A* **2014**, *2*, 7526−7534.

(64) Guo, L.; Jin, X.; Wang, X.; Yin, L.; Wang, Y.; Yang, Y.-W. J. M. Immobilizing polyether imidazole ionic liquids on ZSM-5 zeolite for the catalytic synthesis of propylene carbonate from carbon dioxide. *Molecules* **2018**, *23*, No. 2710.

(65) Lin, X.; Ling, X.; Chen, J.; Li, M.; Xu, T.; Qiu, T. J. G. C. Self-solidification ionic liquids as heterogeneous catalysts for biodiesel production. *Green Chem.* **2019**, *21*, 3182−3189.

(66) Li, C.-J.; Chen, L. Organic chemistry in water. *Chem. Soc. Rev.* **2006**, *35*, 68−82.

(67) Chakraborti, A. K.; Roy, S. R. On catalysis by ionic liquids. *J. Am. Chem. Soc.* **2009**, *131*, 6902−6903.

(68) Benaglia, M. *Recoverable and Recyclable Catalysts*; John Wiley & Sons, 2009.

(69) Saffar-Teluri, A. Boron trifluoride supported on nano-SiO_2: an efficient and reusable heterogeneous catalyst for the synthesis of bis(indolyl)methanes and oxindole derivatives. *Res. Chem. Intermed.* **2014**, *40*, 1061−1067.

(70) Kothandapani, J.; Ganesan, A.; Ganesan, S. S. Magnetically separable sulfonic acid catalysed one-pot synthesis of diverse indole derivatives. *Tetrahedron Lett.* **2015**, *56*, 5568−5572.

(71) Polshettiwar, V.; Varma, R. S. Nanoparticle-supported and magnetically recoverable palladium (Pd) catalyst: a selective and sustainable oxidation protocol with high turnover number. *Org. Biomol. Chem.* **2009**, *7*, 37−40.

(72) Zhang, Z.; Zhang, F.; Zhu, Q.; Zhao, W.; Ma, B.; Ding, Y. Magnetically separable polyoxometalate catalyst for the oxidation of dibenzothiophene with H_2O_2. *J. Colloid Interface Sci.* **2011**, *360*, 189−194.